Unified Pulsed Laser Range Finder and Velocimeter using Ultra-Fast Time-To-Digital Converter

Sh. Mohammad Nejad* and S. Olyaee**

Abstract: In this paper, we present a high accuracy laser range finder and velocimeter using ultra-fast time-to-digital converter (TDC). The system operation is based on the measuring the round-trip time of a narrow laser pulse. A low-dark current high-speed PIN photodiode is used to detect the triggered laser beam and to produce start signal. The pulsed laser diode generates 45W optical power at 30ns duration time and 905nm wavelength. A high-responsivity avalanche photodiode (APD) detects the reflected beam from the target. An optical head including beam splitter, lenses and optical filters is also designed and implemented. The signal conditioner of the system includes pre- and post-amplifiers, comparator, opto-isolators and monostable. By using a 3MV/W reach-through structure avalanche photodiode and a wideband pre-amplifier, the pre-amplifier output reaches 15.9mV, resulting from the minimum detectable optical power. The APD temperature and as a result its responsivity is controlled by a thermoelectric controller unit. The start and stop signals from PIN and APD are led to the time-to-digital converter to count the round-trip time of the laser beam. The system is tested by a retro-reflector as a target for 30-1200m distances. The resolutions of the distance and velocity measurement are limited to 18.75mm and 1.2m/s, respectively. In the worst condition, the minimum reflected optical power is limited to about 5.3nW in 1.2km distance.

Keywords: APD, Laser Velocimeter, Pulsed Laser Diode, Range Finder, TDC.

1 Introduction

Laser velocimeters and range finders are being widely used in many industrial, military and medical applications [1]-[8]. Most of them such as flowmeters are based on the Doppler effect [9]-[13]. Time-of-flight (TOF) method is commercially used to measure the distance or displacement in the long range [14]. The most important limitation in the distance measurement with high resolution is the clock pulse counter.

Using an ultrasonic wave, the round-trip time is considerable value, because of its low velocity [15]-[17]. However, if the light beam is used as a carrier, the time is so small that a high resolution counter should be applied to measure that. If a 30MHz clock pulse is applied to measure the round-trip time of the laser beam, a ±5m resolution is obtained [14]. Obviously, this resolution is not enough to measure distances up to 1km. As a result, a good measuring velocity can not be achieved.

In this paper we utilize an ultra-fast time-to-digital converter with 8GHz clock pulse. The distance resolution resulting from clock pulse counter is limited to several millimeters. Consequently, a good resolution in the velocity measurement is obtained.

2 Laser Velocimeter Based on the TOF Method

The basic principle of time-of-flight velocimeter and range finder is based on the measuring the round-trip time of a short powerful laser pulse. The powerful laser pulse can be achieved by reducing the pulse width of the output signal using the Q-switched laser cavity [14]. It can also cause to increase the signal-to-noise ratio. The traveled laser beam is divergent and the reflected beam distributes in the hemisphere pattern as shown in Fig. 1. Since the laser beam travels a distance of 2R, the receiving power is usually very small. The received optical power is given by [6]:

Iranian Journal of Electrical & Electronic Engineering, 2009.
Paper is first received 2 Nov. 2008 and in revised form 7 Apr. 2009.
* The Author is with the Nanoptronics Research Laboratory, Department of Electrical Engineering, Iran University of Science and Technology, Narmak, 16846, Tehran, Iran.
E-mail: shahramm@iust.ac.ir
** The Author is with the Department of Electrical Engineering, Nano-Photonics and Optoelectronics Research Laboratory, Shahid Rajaee Teacher Training University, Lavizan, 16788, Tehran, Iran.
E-mail: s_olyaee@srttu.edu

$$P_r = \frac{\rho d_{TX}^2 d_T^2 \alpha^2}{8R^2 \left(R\theta_{v_2} + d_{TX}\right)^2} P_t \qquad (1)$$

Where P_t is the output power from the laser cavity, d_{TX} is the transmitter lens diameter, d_T is the target diameter, θ_{v_2} is the divergence angle, ρ is the target reflectivity at laser wavelength and α is the absorption coefficient of the medium. If $d_{TX} \ll R\theta_{v_2}$, Eq. (1) can be rewritten as:

$$P_r = \frac{\rho d_{TX}^2 d_T^2 \alpha^2}{8R^4 \theta_{v_2}^2} P_t \qquad (2)$$

Therefore, the reflected power is strongly reduced by increasing the distance, and consequently, a high-responsivity low-noise wideband photodetector and pre-amplifier is needed to detect the reflected beam.

A block diagram of the unified laser range finder and velocimeter based on the TOF method is represented in Fig. 2. The output beam from the transmitter is directed toward the target and its reflection is collected by the receiver optics. A START signal is simultaneously introduced to the processing circuit through a PIN photodiode joined by the pulsed laser diode. By receiving the START signal, a counter is activated until the STOP signal is received. After traveling a distance of 2R, the laser beam through the optics arrives on the APD having high responsivity and a short rise time. In order to stop the counter, the APD photocurrent is converted into a voltage signal and is amplified. The distance between the target and the transmitter in terms of the clock pulse frequency (f_{clk}) is calculated as:

$$R = \frac{cN_c}{2f_{clk}} \qquad (3)$$

where N_c is the counted digits (between the START and the STOP signals) and c is the speed of light. In accordance to Eq. (3), the resolution of the system resulting from the clock pulse counter becomes,

$$\delta_r = \frac{c}{2f_{clk}} \qquad (4)$$

By sampling the distance of movable target, the target velocity is also obtained as:

$$v = \frac{\Delta R}{T_s} \qquad (5)$$

where T_s is the sample time or repetition rate of the laser.

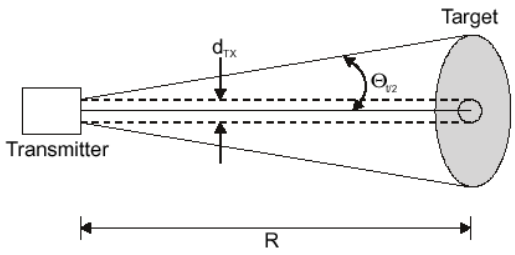

Fig. 1. The laser beam divergence.

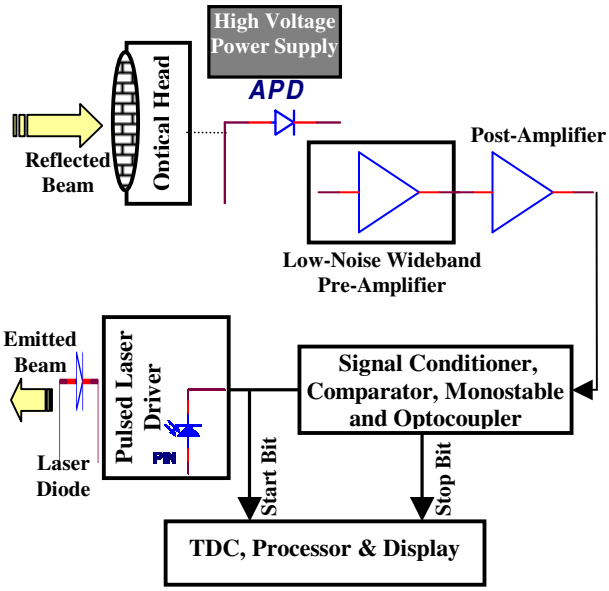

Fig. 2. The schematic representation of a unified time-of-flight laser range finder and velocimeter.

3 Design and Implementation

3.1 Pulsed Laser Driver

The main function of the pulsed laser driver is to produce a relatively powerful short period pulse, to adjust its repetition rate and also to generate the START signal. The starting signal is produced by a silicon PIN photodiode having dark current I_d = 10nA and a rise time τ_r=5ns . When the laser is triggered and the laser beam is directed out of the cavity, a current pulse is produced by the PIN photodiode and is then fed to the processing section to start the counter.

As shown in Fig. 2, a 905nm pulsed laser diode is used to produce the high peak output power in the transmitter. The center wavelength of PGEW3S09, constructed based on the multiple quantum well, is well-matched to the peak response of Si avalanche photodiode [18]. The output optical power of the laser diode is 45W and the maximum forward current is $25A_p$. The laser driver produces impulses with ultra-low duty cycles (30ns high at 6.25ms duration results in about $0.48\times10^{-3}\%$ duty cycle). The transmitted optical power is increased by reduction of current pulse width, and consequently, the received power can be increased. Fig. 3 represents the pulsed laser driver.

At first, a proper train pulse with 160Hz frequency is generated by using a rectangular generator. The output signal is led to the differentiator circuit and as a result the signal with narrow pulse width is generated. To reach the minimum rise time, a high-speed comparator is also designed.

3.2 Pre- and Post-Amplifiers

A small fraction of the main reflected beam from the target is received by the optical receiver and is focused on an avalanche photodiode. As shown in Fig. 2, the

avalanche photodiode is used to detect the reflected beam and to produce STOP signal. In the worst condition, the minimum reflected optical power is limited to about 5.3nW in 1.2km distance (The maximum transmitted optical power is 45W). Therefore, the avalanche photodiode should have high responsivity and minimum noise [19]-[21]. In this system, we use an integrated circuit including a high-responsivity low-noise reach-through structure avalanche photodiode (C30659) and a FET wideband transimpedance amplifier [22]. Fig. 4a shows the transimpedance pre-amplifier. An emitter follower is used as the output buffer stage. To obtain the wideband characteristic,the output should be AC (capacitively) coupled to a 50Ω termination. A temperature compensated HV power supply is also used to maintain responsivity constant over temperature.

The C30659 responsivity and bandwidth are equal to 3000kV/W at 900nm wavelength and 50MHz, respectively. Because this APD includes a built-in current-to-voltage converter (pre-amplifier), its responsivity is denoted by kV/W. As a result, the minimum output signal can be calculated as:

$$V_o = \Re P_{inc} = 15.9\,mV \qquad (6)$$

where $\Re$ is the responsivity and P_{inc} is the optical power focused on the avalanche photodiode.

The output signal of the emitter follower is fed to a post-amplifier. A monolithic amplifier (MAR) amplifies the output signal of the emitter follower as shown in Fig. 4b. Input impedance of MAR is equal to 50Ω which is in good agreement with the output impedance of the pre-amplifier [23]. The voltage supply through the RFC is led to the output which is used to prevent the supply noise.

The amplifier output is implied to a comparator to allow the increase of the output to the TTL level. The signal comparison level due to the minimum received power (5.3nW) at the end of the pre-amplifier is considered to be 14mV. This in turn will reduce the system's noise effects. The noise level equal to 5.3nW optical power can not change the comparator output. By using a proper shielding and grounding, and reducing the ground resistivity, the powers less than 5.3nW can also be detected. The pulse width of the signal is then increased by a mono-stable and the STOP signal of the counter is fed to the opto-coupler. So it is fed to the digital section of the system.

3.3 High Voltage Power Supply

To reach a proper responsivity of APD, the 400V reverse bias of avalanche photodiode should be generated and stabilized. Fig. 4c represents the schematic diagram of stabilized high voltage power supply. The Colpitts oscillator produces a sinusoidal signal and then its amplitude is amplified by using a transformer. The LC circuit considerably reduces the signal ripple. It should be noted that the output current of high voltage power supply is limited to a few microamperes. The maximum measured ripple of power supply is as small as 0.01%.

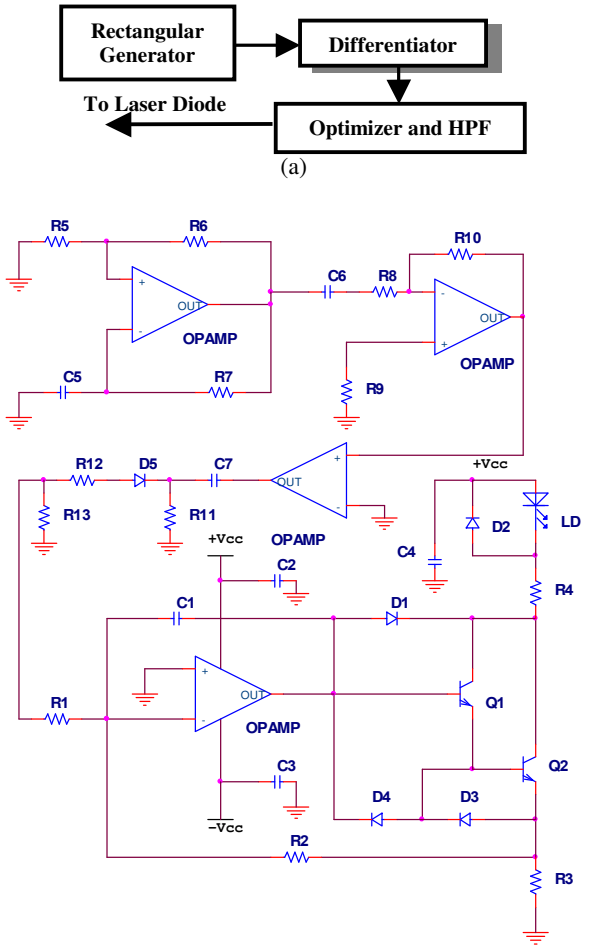

Fig. 3. (a) The block diagram and (b) schematic diagram of the pulsed laser driver.

On the other hand, it is required that the pre-amplifier gain to be proportional to the received optical power. This can be accomplished by variation of the APD responsivity with respect to the biasing voltage. Fig. 5a shows the variation of APD responsivity in terms of the operating voltage [22]. The variation of the bias in the range of 200-425V (T = 22ºC) causes the responsivity to vary between 320kV/W to 3MV/W.

3.4 Thermoelectric Controller

An important section of the APD circuits is the APD temperature controller that is shown in Fig. 5b [24]. The responsivity variation as a function of temperature is important in design of thermoelectric controller (TEC). The thermistor resistance as a function of temperature is given by [24]-[25]:

$$T = \left[\frac{1}{3940}\ln 10^{-1} R_T + \frac{1}{298}\right]^{-1} \qquad (7)$$

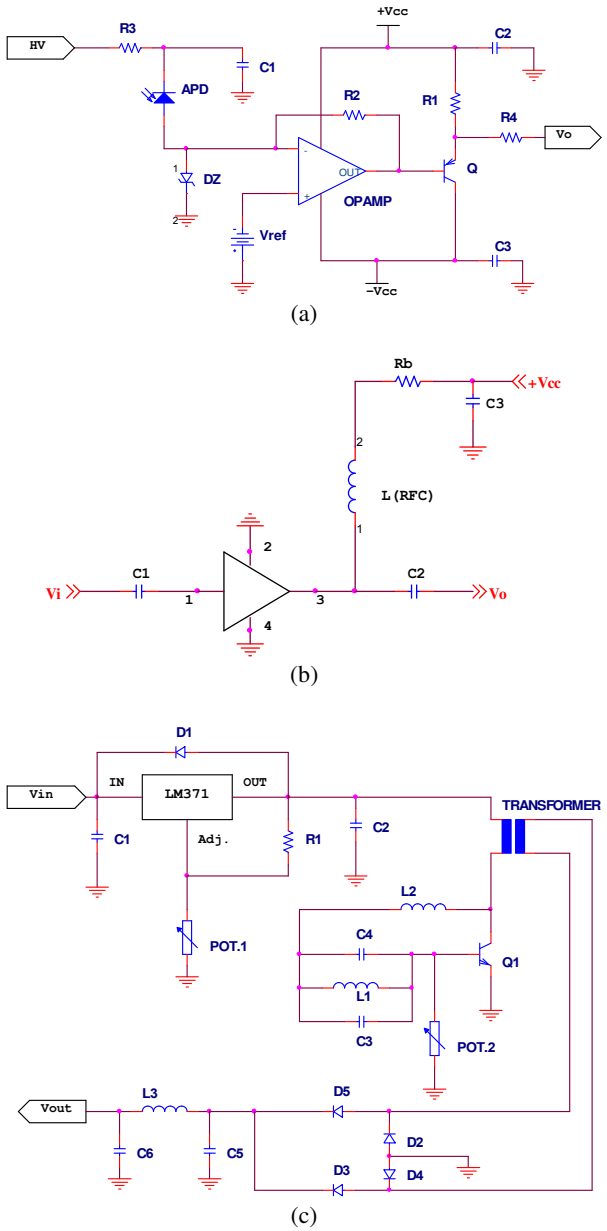

Fig. 4. The schematic diagram of (a) transimpedance pre-amplifier, (b) the post-amplifier based on the wideband monolithic amplifier and (c) the high voltage power supply.

At 0 ºC, thermistor resistance will be up to 33.5 kΩ and we will have,

$$R_3+R_4=\frac{R_T R_2}{R_1} \quad , \quad R_4=560\Omega \qquad (8)$$

3.5 Time-To-Digital Converter

In the present system, an ultra-fast counter as time-to-digital converter (TDC) is used to measure the round-trip time of the laser beam. The TDC-GP1 can be utilized either 2 channels with 250ps resolution or 1 channel with 125ps resolution. A main ALU of counter stores the measurement results into the result registers (8 registers at 16 bit). The result registers should be read out via microcontroller interface. The schematic diagram of the time-to-digital converter is shown in Fig. 6. The analogue section and digital section (including start and stop paths) are isolated by two optocouplers.

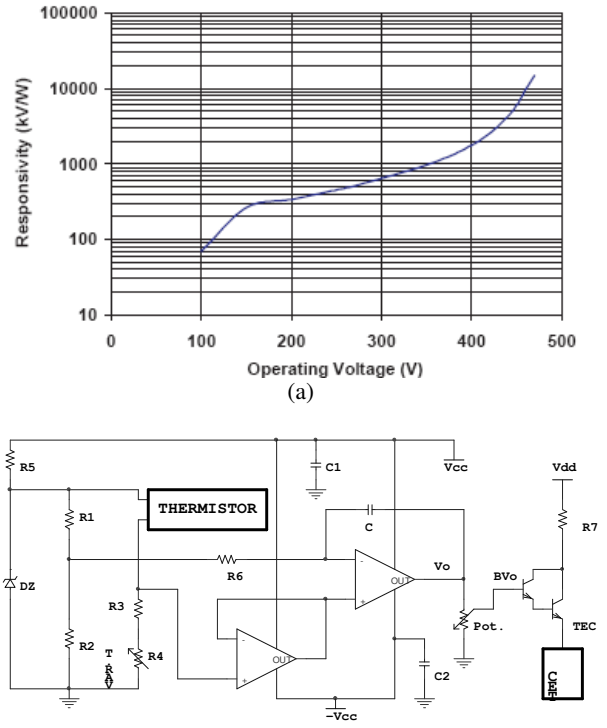

Fig. 5. (a) The variation of APD responsivity in terms of the operating voltage [22] and (b) the thermoelectric controller [24].

Considering the 8 GHz clock pulse frequency, the obtained resolution from Eq. (4) becomes 18.75 mm. Also, in the worst condition, the error of measured target velocity is limited to 6 m/s. The accuracy of velocity and distance measurement can be improved by using an appropriate algorithm. In order to match the repetition rate of the laser, the accuracy of velocity measurement is increased to about 1.2 m/s by omitting the out of range data. According to the repetition rate of 160 Hz, we have 160 samples per second and 480 samples for each display refreshment. The obtained data from the counter is sent to the microcontroller and proper phrase is presented on the LCD. If for any reasons, the one cycle output signal of the laser is received by the detector, an ERROR signal will be produced. The lack of receiving signal could have many reasons such as the target is located very far, the beam is being greatly absorbed by the transmitting media, the target being a very absorbing object and so on. Also, if the measured distance is not in the selected range, a PAUSE phrase will be shown on the LCD. Since the delay time related to the electronic circuits in the START and STOP paths are not equal, it is necessary that this time difference which causes some deviations in the measurements, to be eliminated. The time

difference could be eliminated either by hardware or software. It should be noted that the TDC can be calibrated via direct command or automatically via start/stop inputs. In the present system, we use a calibration unit along START path with appropriate initialization of TDC. Hence, for closest target (at 30 m distance) the delay time of START and STOP paths are equal.

3.6 Optical Section

The received optical power should be collected, focused and filtered by an optical head. A proper optical head not only collects and focuses the incident beam, but also it could be designed to filter and eliminate the undesired radiation arriving at the receiver. The optical head of the system, designed by the Zemax software, is constructed as shown in Fig. 7 [24]. The reflected beam of the target is focused on the avalanche photodiode by a lens and an optical filter.

The lens is made of a crown glass having an absorbing range of 10 μm and is covered with an anti-reflection layer of MgF_2 with 1.38 reflectivity. The thickness of the anti-reflection layer is about 0.18 μm. This layer is not only to optimize the detectivity, but also acts as a proper optical filter. The reason for using the above mentioned glass is that it is not soluble in water, it has the shortest (1 μm) passing stripe and is a very good absorbent of the wavelengths above 3.5 μm (the thermal radiation wavelengths). As for the interference filters used in this design, with the use of thin layers of dielectric materials of different thickness, one can design a Fabry-Perot filter. The transfer matrix of the beam through the layer can be written as follows:

$$\begin{bmatrix} A & iB \\ iC & D \end{bmatrix} = \prod_{m=1}^{N} M_m = \prod_{m=1}^{N} \begin{bmatrix} \cos\delta_m & \frac{i}{\mu_m}\sin\delta_m \\ i\mu_m \sin\delta_m & \cos\delta_m \end{bmatrix} \quad (9)$$

$$\delta_m = \frac{2\pi n_m d_m \cos\theta_m}{\lambda} \quad (10)$$

$$\text{for polarization P: } \mu_m = \frac{n_m}{\cos\theta_m} \quad (11)$$

$$\text{for polarization S: } \mu_m = n_m \cos\theta_m \quad (12)$$

$$P_e = \frac{4\mu\mu_S}{(\mu A + \mu_S D)^2 + (\mu_o \mu_S B + C)} \quad (13)$$

where n is the refractive index, A is the radiation angle, d is the layer thickness, m stands for the layer number and P_e is the emission power.

The glass used for the substrate has n_s = 1.5. Also the MgF_2 having n = 1.38 is used as the layer of low refractive index and ZnS with n = 2.29 is used as the high refractive index layer. The materials selected for layers have relatively high melting temperatures. They are relatively tough and can not be dissolved in water. In the simulation carried out for 5 layers, a quality factor Q_1 = 1.59 could be obtained. As shown in Fig. 8, by repeating the semi-layers, a filter having $Q = Q_1Q_2$ = 2.53 was obtained. On the other hand, since a thin metal layer on a transparent dielectric is a good reflector for IR and also is a good transmitter for visible radiation, a direct observation of the target is possible.

4 Noise Analysis in Unified Laser Range Finder and Velocimeter

The resolution of distance and velocity measurement can be limited by the system noise. Because the minimum received optical power is as small as several nanowatts, the signal-to-noise ratio (SNR) should be enough. In the pulsed laser range finder and velocimeter, the optical noise can be greatly reduced by designing and implementing proper optics. The main internal noise is the one created in the receiver STOP channel. Due to the isolation of the analogue section from other parts, the noise effect of the other parts is being curtailed. The switching noise of the laser driver is being eliminated by electromagnetic interference (EMI) filters. Furthermore, the digital noise is eliminated by separating the source and the ground from the analogue section of the receiver (see Fig. 6). However, the main noise related to the receiver channel is the noise of the preamplifier which is given by [24], [26]:

$$\langle i_n^2 \rangle = \frac{4kT}{Z_i}\left(\frac{\pi}{2}\Delta f_i\right) \quad (14)$$

where k is the Boltzmann constant, T is the absolute temperature, Z_i is the input impedance of the preamplifier and Δf_i is the system bandwidth. The equivalent optical power will then become [24], [26],

$$\Im = \frac{\langle i_n \rangle}{R} \quad (15)$$

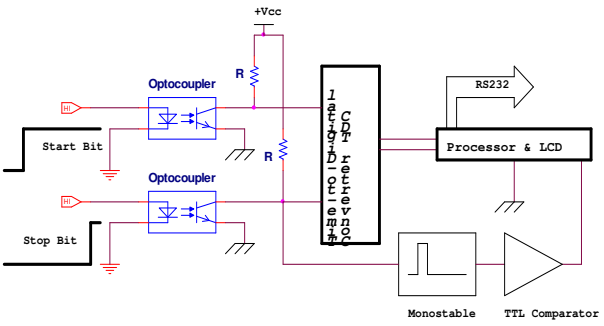

Fig. 6. The schematic diagram of the time-to-digital converter.

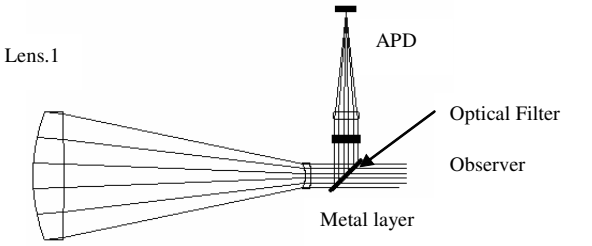

Fig. 7. The range finder optics designed by Zemax software [24].

The signal-to-noise ratio is one of the main elements determining the resolution of the system [27]. For present system, the relation between the resolution of the system and the SNR could be presented by [3]:

$$\delta_d = \frac{c}{2}\frac{\langle n \rangle}{dU/dt} = \frac{0.35c}{2\Delta f_i.SNR} \qquad (16)$$

where dU/dt is the slope of the time dependent pulse and $\langle n \rangle$ is the rms noise value. For repetition rate of N, Eq. (16) can be rewritten as:

$$\delta_d = \frac{0.35c}{2\sqrt{N}\Delta f_i.SNR} \qquad (17)$$

It should be noted that the signal-to-noise ratio is considered for the STOP path. The START path signal is so large that eliminates the effect of the SNR (the START path begins from the PIN photodiode located behind the laser). If the SNR of the START path is small, Eq. (17) could be changed as:

$$\delta_d = \frac{0.35c}{2\sqrt{N}\Delta f_i}\left[\frac{1}{SNR^2_{START}} + \frac{1}{SNR^2_{STOP}}\right]^{1/2} \qquad (18)$$

In practical situation, the SNR_{START} is larger and hence the total resolution will be limited to that of the digital section. On the other hand the signal-to-noise ratio is given by:

$$SNR = \frac{i_S}{i_n} = \frac{M\Re P_{inc}}{\left[2q\left(K_{TP}P_{inc}\Re M^2 F(M) + i^2_{na}\right)\right]^{1/2}} \qquad (19)$$

where K_{TP} = 0.5, M is the internal gain of the avalanche photodiode and F(M) is the excess noise factor. The excess noise factor in terms of the effective ionization ratio is calculated by:

$$F(M) = M\left[1-(1-K_{eff})\left(\frac{M-1}{M}\right)^2\right] \qquad (20)$$

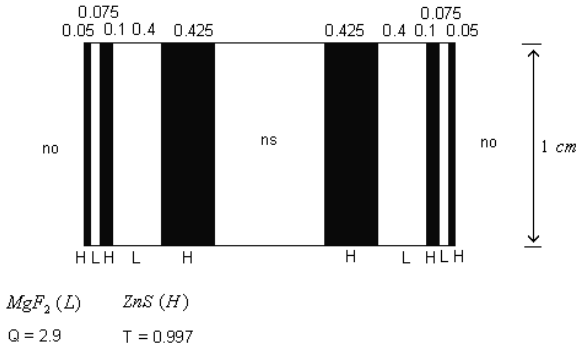

Fig. 8. The designed filter from layers of ZnS and MgF_2 with quality factor = 2.53 [24].

Table 1. The specification of pulsed laser driver.

Parameter	Value	Unit
Voltage power supply	±14	V
Maximum current source (continuous)	40	mA
Frequency	160	Hz
Impulse peak to voltage-to-current converter	14	V
Measured pulse width	35	ns
Measured peak current	8	A
Maximum laser power	45	W

5 Results

The output current of pulsed laser driver is shown in Fig. 9. The pulse width is less than 30 nsec. and the current amplitude is about 8A. Table 1 presents pulsed laser driver specifications.

As mentioned previously, the APD responsivity can be adjusted by its reverse bias voltage. Therefore, the responsivity should not be varied by other parameters such as thermal fluctuations. Using a TEC, the temperature of APD is fixed. Fig. 10 shows the variation of APD responsivity in terms of temperature. The linear region of TEC output is between - 0.14 to -1.36V. As a result, by changing the thermistor resistance between 11.62 to 30.63 kΩ, one can adjust temperature from 2 to 21 ºC. On the other hand, the maximum measured ripple in high voltage power supply is limited to 0.01%, and therefore, the APD responsivity is fixed.

The transmission curve of top-layer of the optical filter is presented in Fig. 11(a). Considering thickness and refractive index errors equal to 0.01, the transmission curve is simulated as shown in Fig. 11(b). In addition the total transmission curves (top- and bottom-layers) are respectively shown in Fig. 12. With respect to the pulsed laser wavelength, the transmission coefficient is about 99%.

Fig. 13(a) shows the resolution in terms of the signal-to-noise ratio. Considering the resolution of the digital section obtained from Eq. (4) to be 18.75mm, the minimum required signal to noise ratio obtained for the worst case (N = 1) from Eq. (16) becomes 28.

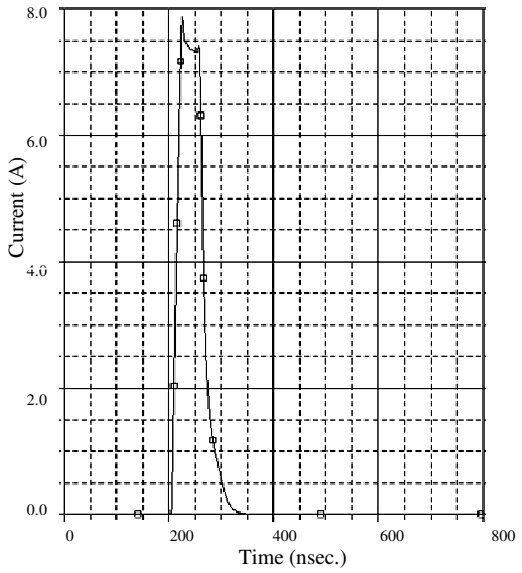

Fig. 9. The output current of the laser driver.

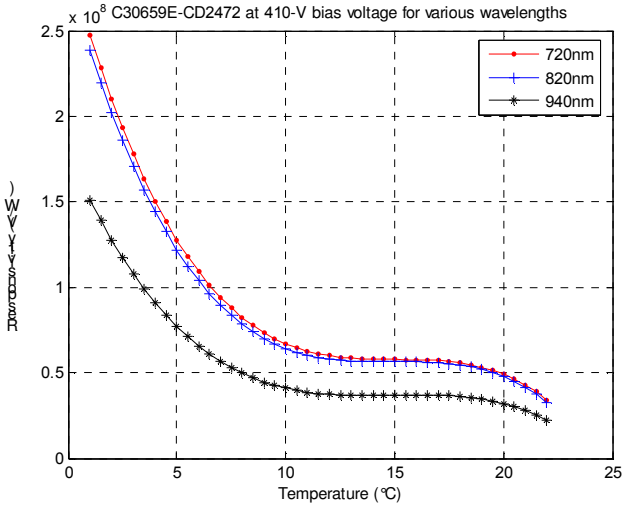

Fig. 10. The APD responsivity in terms of temperature.

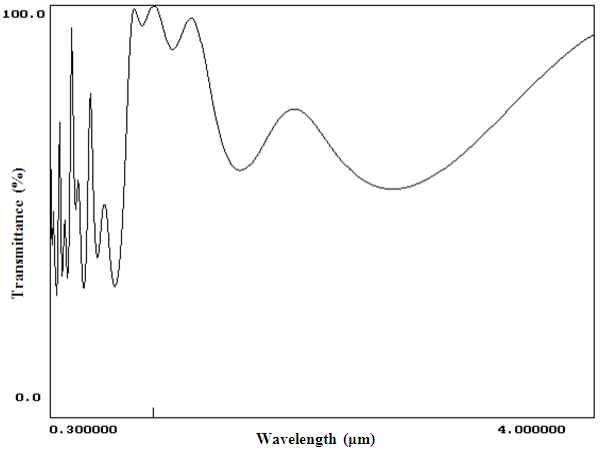

(a)

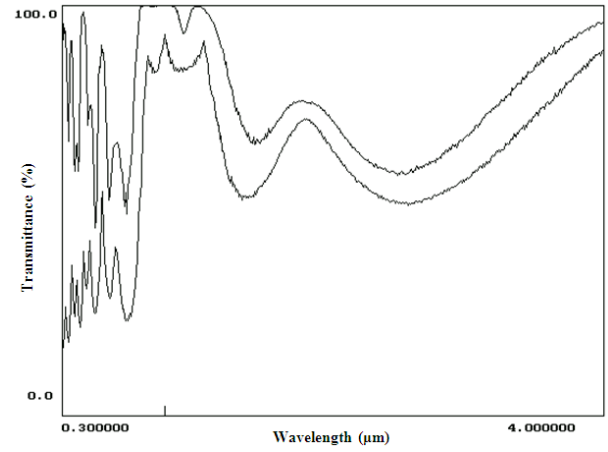

(b)

Fig. 11. The transmission curve of top-layer (a) ideal curve and (b) with 0.01 errors in refractive index and thickness.

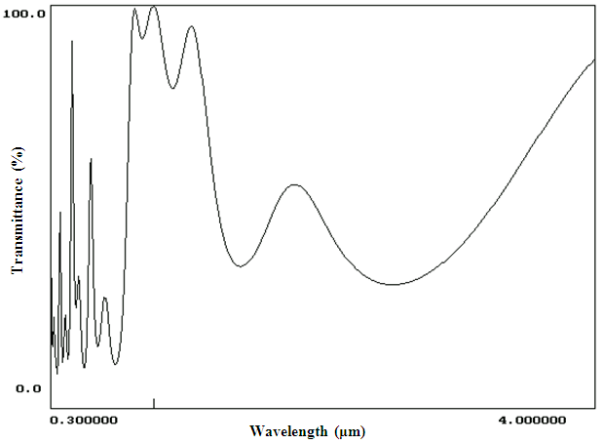

(a)

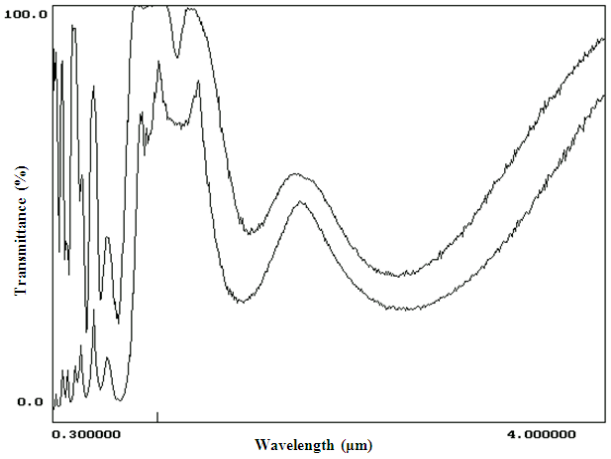

(b)

Fig. 12. The total transmission curve (a) ideal curve and (b) with 0.01 errors in refractive index and thickness.

Fig. 13(b) presents the excess noise factor variation in terms of M for different effective ionization ratio (K_{eff}). As can be seen, when effective ionization ratio is

decreased, the noise factor will be considerably increased. Using a Slik structure for avalanche photodiode instead of reach-through and beveled-edge APD, the K_{eff} can be decreased up to 0.002 [28]-[30]. On the other hand with reference to Fig. 13(b), the excess noise factor increases with M, which it is undesirable. Fig. 13(c) shows the signal to noise ratio in terms of M, which for M = 7.9 the maximum SNR is obtained.

The implemented pulsed laser range finder and velocimeter using the ultra-fast time-to-digital converter is shown in Fig. 14. The implemented system is successfully tested by a retro-reflector target ($\rho \geq 0.9$) for the best results in the range of 30m to 1200m.

6 Conclusion

Design, simulation and implementation of a laser velocimeter and range finder based on the ultra-fast time-to-digital converter have been presented. All optical and electronic sections were implemented and successfully tested. The electronic section includes high-voltage power supply to produce low-ripple reverse bias for APD, wideband low-noise pre- and post-amplifiers, comparator, monostable, time-to-digital converter and processor, thermoelectric controller and optocouplers. The APD responsivity can be varied by reverse bias voltage produced by high voltage power supply. The 30 nsec. laser beam and 8 GHz clock pulse counter cause the distance resolution reaches about 18 mm in over range and the target velocity resolution is limited to 1.2 m/sec., in the worst condition.

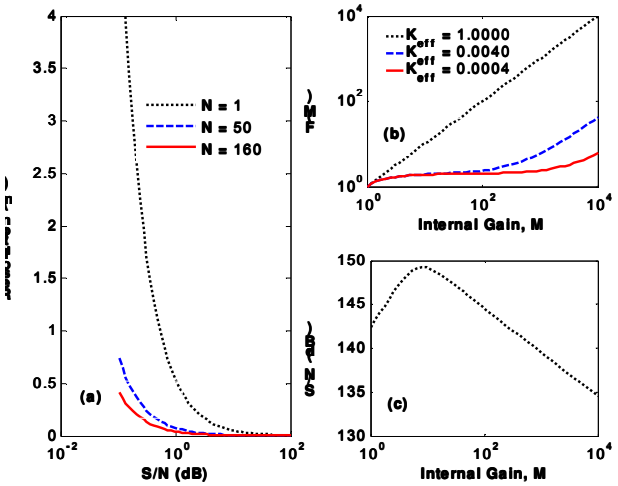

Fig. 13. (a) Receiver resolution in terms of the signal-to-noise ratio, (b) the excess noise factor variation in terms of M for different effective ionization ratio and (c) the signal to noise ratio in terms of M.

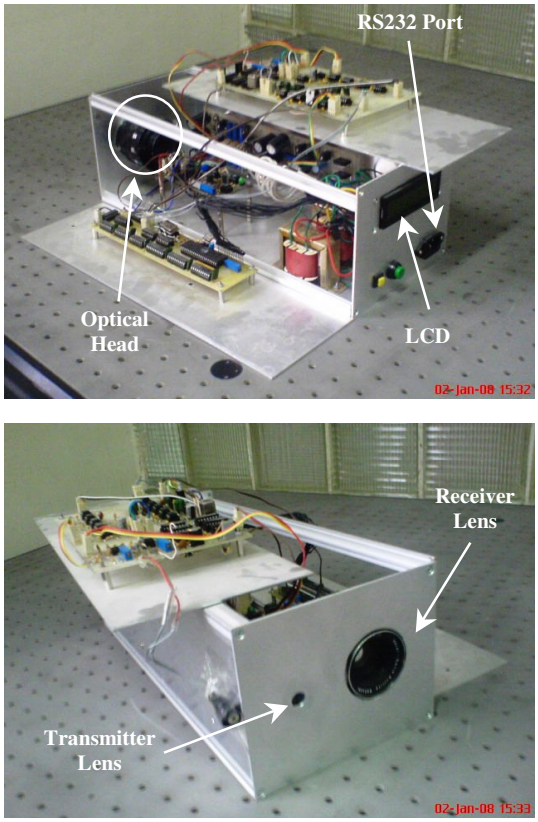

Fig. 14. The unified pulsed laser range finder and velocimeter.

References

[1] Mohammad Nejad S. and Mirsaeedi H., "Altitude measurement using laser beam reflected from water surface", *International Journal of Engineering Science*, Vol. 1, No.1, 2005.

[2] Mohammad Nejad S. and Mohajeri I., "Design and simulation of a high resolution FMCW-like laser range finder", *Proceedings of the 13th Iranian Conference on Electrical Engineering*, pp. 372-377, 2005.

[3] Maatta K., Kostamovaara J. and Myllyla R., "Profiling of hot surfaces by pulsed time of flight laser range finder techniques", *Appl. Opt.*, Vol. 32, No. 27, pp. 5334-5342, 1993.

[4] Martinez J. C., "A robust photo-interferometric technique to obtain the refractive index and thickness of non-absorbing stand-alone films", *Meas. Sci. Tech.*, Vol. 11, pp. 1138-1144, 2000.

[5] Jakobsen M. L., Osten S., Kitchen S. R., Dam-Hansen C. and Hanson S. G., "Multiple-beam time-of-flight sensor based on a vertical cavity surface emitting laser diode array", *Meas. Sci. Technol.*, Vol. 14, pp. 329-335, 2003.

[6] Kilpela A., "Pulsed time-of-flight laser range finder techniques for fast, high precision

measurement applications", *Oulu University Press*., Oulu, Finland, 2004.

[7] Makynen A., "Position-sensitive devices and sensor systems for optical tracking and displacement sensing applications", *Oulu University Press*., Oulu, Finland, 2000.

[8] Allen J., Frame J. R. and Murray A., "Microvascular blood flow and skin temperature changes in the fingers following a deep inspiratory gasp" *Physiol. Meas*., Vol. 23, pp. 365–373, 2002.

[9] Czarske J., "A miniaturized dual-fibre laser Doppler sensor*", Meas. Sci. Technol*. Vol. 12, pp. 1191-1198, 2001.

[10] Esen F. and Esen H., "Detrended fluctuation analysis of laser Doppler flowmetry time series: the effect of extrinsic and intrinsic factors on the fractal scaling of microvascular blood flow", *Physiol. Meas*, Vol. 27, pp. 1241–1253, 2006.

[11] Guler I. and Guler N. F., "The electronic detail of a pulsed Doppler blood flow measurement system", *Meas. Sci. Technol*, Vol. 1, pp. 1087-1092, 1990.

[12] Logeana E., Geiserb M. H. and Riva C. E., "Laser Doppler instrument to investigate retinal neural activity-induced changes in optic nerve head blood flow", *Optics and Lasers in Engineering*, Vol. 43, pp. 591-602, 2005.

[13] Beutner T. J., Elliott G. S., Williams G. W., Baust H. D., Crafton J. and Carter C. D., "Forebody and leading edge vortex measurements using planar Doppler velocimetry", *Meas. Sci. Technol.*, Vol. 12, pp. 378-394, 2001.

[14] Mohammad Nejad S. and Olyaee S., "A new high accuracy time-of-flight range finder with Q-switching Nd:YAG laser", *Proceedings of the 12th Iranian Conference on Electrical Engineering,* Ferdowsi University of Mashhad, pp. 121-126, May 2004.

[15] Meile T., Cesare G. D., Blanckaert K. and Schleiss A. J., "Improvement of acoustic Doppler velocimetry in steady and unsteady turbulent open-channel flows by means of seeding with hydrogen bubbles", *Flow Meas. Ins*., Vol. 19, No. 3, pp. 215-221, 2008.

[16] Tezuka K., Mori M., Suzuki T. and Kanamine T., "Ultrasonic pulse Doppler flow meter application for hydraulic power plants", *Flow Meas. Ins.*, Vol. 19, No. 3, pp. 155-162, 2008.

[17] Liang W. and Que P. W., "Maximum non-Gaussianity parameters estimation of ultrasonic echoes and its application in ultrasonic non-destructive evaluation", *Meas. Sci. Technol.,* Vol. 18, pp. 3743-3750, 2007.

[18] PGEW series, "905 nm plastic pulsed laser diode", http://www.optoelectronics. perkinelmer. com, *Perkin Elmer Inc*., Accessed February 2008.

[19] Hollenhorst J. N., "A theory of multiplication noise", *IEEE Trans. Electron Devices*, Vol. 37, No. 3, pp. 781-788, 1990.

[20] Redus R. and Farrell R., "Gain and noise in very high gain avalanche photodiodes: theory and experiment", *SPIE*, Vol. 2859, pp. 288–297, 1996.

[21] Hakim N. Z., Saleh B.E.A. and Teich M. C., "Generalized excess noise factor for avalanche photodiodes of arbitrary structure", *IEEE Trans. Electron Devices*, Vol. 37, No. 3, pp. 599-610, 1990.

[22] C30659E series, "Silicon and InGaAs APD", www.http://optoelectronics.perkinelmer.com, *Perkin Elmer Inc*., Accessed February 2008.

[23] MAR, "Monolithic amplifiers", http://www.minicircuits.com, *Mini-Circuits Inc*, Accessed February 2008.

[24] Mohammad Nejad S. and Olyaee S., "Low-noise high-accuracy TOF laser range finder", *Am. J. Appl. Sci*., Vol. 5, No. 7, pp. 755-762, 2008.

[25] Refaat T. F., Luck W. S., and DeYoung R. J., "Temperature control of avalanche photodiode using thermoelectric cooler", *NASA/TM1999, Old Dominion University*, Norfolk, Virginia, October 1999.

[26] Mohammad Nejad S. and Olyaee S., "Cross-talk and intermediate frequency deviation effects on phase-shift range finder", *International Journal of Engineering Science*, Vol. 13, No. 1, pp. 167-177, 2002.

[27] Pellegrini S., Buller G., Smith J., Wallace A. and Cova S., "Laser-based distance measurement using picosecond resolution time-correlated single-photon counting", *Meas. Sci. Technol. Vol. 11*, pp. 712-716, 2000.

[28] Refaat T. F., Halama G. E. and DeYoung R. J., "Characterization of advanced avalanche photodiode for water vapor lidar receivers", *NASA/TP2000*, Old Dominion University, Norfolk, Virginia, July 2000.

[29] Refaat T. F., Halama G. E. and DeYoung R. J., "Comparison between super low ionization ratio and reach through avalanche photodiode structures", *Opt. Eng*., Vol. 39, No. 10, pp. 2642-2650, 2000.

[30] Refaat T. F. and Elsayed-Ali H. E., "Advanced Atmospheric Water Vapor DIAL Detection System", *NASA/CR-2000-210301*, Old Dominion University, Norfolk, Virginia, June 2000.

Shahram Mohammad Nejad received his B.Sc. in Electrical Engineering from University of Houston, Houston, USA, in 1981 and M.Sc. and Ph.D. degrees in Semiconductor Material Growth and Lasers from Shizuoka University, Shizuoka, Japan, in 1990 and 1993, respectively. Professor Mohammad Nejad invented the PdSrS laser for the first time in 1992. He has published over 80 scientific papers and books. Currently, he is the Head of Electrical Engineering Department, Iran University of Science and Technology, Tehran, Iran. Also, he is a scientific committee member of Iranian Conference of Electrical Engineering (ICEE), member of Institute of Engineering and Technology (IET) and an IET- CEng. His research interests include semiconductor material growth, quantum electronics, semiconductor devices, optoelectronics, electronic devices and lasers.

Saeed Olyaee was born in Mashhad, Iran, in 1975. He received the B.Sc. degree in Electrical Engineering from University of Mazandaran, Babol, Iran, in 1997 and the M.Sc. and the Ph.D. degrees in Electrical Engineering specializing in Optoelectronics from Iran University of Science and Technology, Tehran, Iran, in 1999 and 2007, respectively. His doctoral dissertation concerned nanometric displacement measurement based on three-longitudinal-mode laser. Currently, he is an Assistant Professor in Department of Electrical Engineering, Shahid Rajaee University, Tehran, Iran. Dr. Olyaee's main research interests include nanodisplacement measurement, optical instrumentation and optoelectronic circuits.